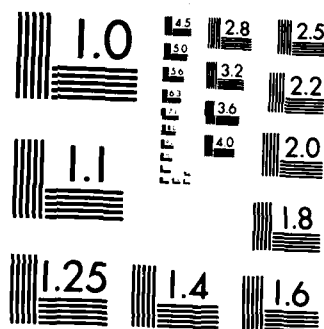


AD-A155 018 CHARACTERISTICS AND SOURCES OF E-REGION IONIZATION IN THE CONTINUOUS AURORA(U) SCT INTERNATIONAL MENLO PARK CA R M ROBINSON ET AL. OCT 84 SRI-ESU-5401 1/1

UNCLASSIFIED AFGL-TR-84-0249 F19628-83-C-0001 F/G 4/1 NL



MICROCOPY RESOLUTION TEST CHART  
NATIONAL BUREAU OF STANDARDS-1963-A

AD-A155 018

DTIC FILE COPY

AFGL-TR-84-0249

**CHARACTERISTICS AND SOURCES OF  
E-REGION IONIZATION IN THE  
CONTINUOUS AURORA**

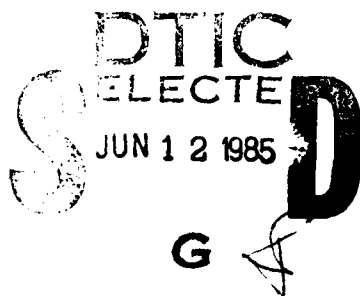
By: ROBERT M. ROBINSON JOHN D. KELLY RICHARD R. VONDRAK

SRI INTERNATIONAL  
333 Ravenswood Avenue  
Menlo Park, California 94025

*Final Report*  
*15 December 1982 to 30 September 1984*

*October 1984*

Approved for public release; distribution unlimited.



*Prepared for:* AIR FORCE GEOPHYSICS LABORATORY  
AIR FORCE SYSTEMS COMMAND  
UNITED STATES AIR FORCE  
HANSCOM AFB, MASSACHUSETTS 01731

85 5 17 01 9

"This technical report has been reviewed and is approved for publication"

*A. Pauline Krukonis*

A. PAULINE KRUKONIS  
Contract Manager  
Ionospheric Effects Branch

*Herbert C. Carlson*

HERBERT C. CARLSON, Chief  
Ionospheric Effects Branch  
Ionospheric Physics Division

FOR THE COMMANDER

*Robert A. Skrivane*

ROBERT A. SKRIVANEK  
Director  
Ionospheric Physics Division

This report has been reviewed by the ESD Public Affairs Office (PA) and is releasable to the National Technical Information Service (NTIS).

Qualified requestors may obtain additional copies from the Defense Technical Information Center. All others should apply to the National Technical Information Service.

If your address has changed, or if you wish to be removed from the mailing list, or if the addressee is no longer employed by your organization, please notify AFGL/DAA, Hanscom AFB, MA 01731. This will assist us in maintaining a current mailing list.

UNCLASSIFIED

SECURITY CLASSIFICATION OF THIS PAGE

AD-A155018

## REPORT DOCUMENTATION PAGE

1a. REPORT SECURITY CLASSIFICATION UNCLASSIFIED			1b. RESTRICTIVE MARKINGS None		
2a. SECURITY CLASSIFICATION AUTHORITY N/A			3. DISTRIBUTION/AVAILABILITY OF REPORT Approved for public release; distribution unlimited.		
2b. DECLASSIFICATION/DOWNGRADING SCHEDULE N/A					
4. PERFORMING ORGANIZATION REPORT NUMBER(S) SRI Project No. ESU - 5401			5. MONITORING ORGANIZATION REPORT NUMBER(S) AFGL-TR-84-0249		
6a. NAME OF PERFORMING ORGANIZATION SRI International		6b. OFFICE SYMBOL (If applicable) N/A	7a. NAME OF MONITORING ORGANIZATION Air Force Geophysics Laboratory (LIS)		
6c. ADDRESS (City, State and ZIP Code) 333 Ravenswood Avenue Menlo Park, CA 94025			7b. ADDRESS (City, State and ZIP Code) Hanscom Air Force Base Bedford, MA 01731		
8a. NAME OF FUNDING/SPONSORING ORGANIZATION AFGL		8b. OFFICE SYMBOL (If applicable) LIS	9. PROCUREMENT INSTRUMENT IDENTIFICATION NUMBER Contract No. F19628-83-C-0001		
8c. ADDRESS (City, State and ZIP Code) Hanscom Air Force Base Bedford, MA 01731 Monitor/A. Pauline Krukonis			10. SOURCE OF FUNDING NOS.		
			PROGRAM ELEMENT NO. 62101F	PROJECT NO. 4643	TASK NO. 07
11. TITLE (Include Security Classification) See Block 16					
12. PERSONAL AUTHOR(S) Robinson, Robert M. and Kelly, John D.; Vondrak, Richard R., Lockheed					
13a. TYPE OF REPORT Final		13b. TIME COVERED FROM 82 Dec 15 TO 84 Sep 30	14. DATE OF REPORT (Yr., Mo., Day) October 1984		15. PAGE COUNT 37
16. SUPPLEMENTARY NOTATION  Characteristics and Sources of E-Region Ionization in the Continuous Aurora (U)					
17. COSATI CODES FIELD GROUP SUB. GR. 0401 170201			18. SUBJECT TERMS (Continue on reverse if necessary and identify by block number) Continuous Aurora, Particle Precipitation, Remote Sensing.		
19. ABSTRACT (Continue on reverse if necessary and identify by block number) The continuous aurora is defined as E-region ionization that is steady in time and uniformly distributed over a large portion of the auroral oval. We have studied the characteristics and sources of ionization in the continuous aurora using data from the Chatanika radar and the DMSP and NOAA satellites. The predominant source of ionization in the continuous aurora is precipitating electrons. The energy distribution of these energetic electrons is approximately Maxwellian. Satellite measurements of electron fluxes can be used to infer the ionospheric electron density along the path of the satellite in the altitude range 90 to 160 km. However, these calculations underestimate the actual electron density when other ionization sources are present. Precipitating protons, in particular, can occasionally produce ionization comparable to that produced by precipitating electrons. Measurements of proton fluxes measured by the NOAA 6 satellite were used to estimate the ionization produced by protons. These estimates were compared with the results of measurements made simultaneously by the Chatanika radar. Calculations based on linear transport theory were found to repro-					
20. DISTRIBUTION/AVAILABILITY OF ABSTRACT UNCLASSIFIED/UNLIMITED <input checked="" type="checkbox"/> SAME AS RPT <input type="checkbox"/> DTIC USERS <input type="checkbox"/>			21. ABSTRACT SECURITY CLASSIFICATION UNCLASSIFIED		
22a. NAME OF RESPONSIBLE INDIVIDUAL A. PAULINE KRUKONIS		22b. TELEPHONE NUMBER (Include Area Code) 617-891-3125		22c. OFFICE SYMBOL AFGL/LIS	

UNCLASSIFIED

SECURITY CLASSIFICATION OF THIS PAGE

BLOCK 19. ABSTRACT (Continued from Page 1)

duce the observed profiles fairly well. In sunlit conditions photoionization can also produce continuous auroral E region ionization. Chatanika radar data were used to examine the dependence of this source on solar zenith angle and solar flux.

Accession For

NTIS GRA&I	<input checked="checked" type="checkbox"/>
DTIC TAB	<input type="checkbox"/>
Unannounced	<input type="checkbox"/>
Justification	

By

Distribution/

Availability Codes

Dist	Avail and/or	Special
A/1		



UNCLASSIFIED

SECURITY CLASSIFICATION OF THIS PAGE

#### ACKNOWLEDGEMENTS

We gratefully acknowledge useful discussions with J. R. Jasperse and J. A. Whalen of the Air Force Geophysics Laboratory and J. R. Sharber of the Florida Institute of Technology. We thank C.-I. Meng of the Applied Physics Laboratory, the Johns Hopkins University, for supplying DMSP data and D. S. Evans of NOAA for supplying data from the NOAA-6 satellite. The site crew of the Chatanika radar operated the radar during the experiments. This work was supported by the Air Force Geophysics Laboratory Contract F19628-83-C-0001 and the Lockheed Independent Research Program.

## CONTENTS

ACKNOWLEDGEMENTS . . . . .	iii
LIST OF ILLUSTRATIONS . . . . .	vii
I INTRODUCTION . . . . .	1
II EXPERIMENTAL TECHNIQUE . . . . .	3
III CHARACTERISTICS OF THE CONTINUOUS AURORA . . . . .	4
IV SOURCES OF THE CONTINUOUS AURORA . . . . .	8
A. Electrons . . . . .	8
B. Protons . . . . .	13
C. Photoionization . . . . .	23
V CONCLUSIONS . . . . .	26
REFERENCES . . . . .	27



## ILLUSTRATIONS

1.	Electron Density as a Function of Latitude and Altitude Measured by the Chatanika Radar on 7 March 1981 . . . . .	5
2.	Superimposed Electron Density Measurements from the Aurora Shown in Figure 1 . . . . .	7
3.	Calculated Values of $n_{\max}^E$ , $f_o^E$ , and $h_{\max}^E$ Resulting from Precipitating Electrons with Maxwellian Energy Distributions . . . . .	9
4.	Comparison of the Range of $n_{\max}^E$ and $h_{\max}^E$ Found in the Morning- and Evening-Sector Continuous Auroras . . . . .	10
5.	Comparison of Electron Density Measured by the Chatanika Radar with that Computed from Simultaneous and Coincident DMSP Measurements of Precipitating Electron Fluxes . . . . .	12
6.	Two Examples of Chatanika Radar Measurements of Ionization in Proton Aurora . . . . .	14
7.	A Continuous Auroral E-Layer Produced Entirely by Pre- cipitating Protons . . . . .	15
8.	Electron Density at 130-km Altitude as a Function of Invariant Latitude and Local Time Constructed from Radar Measurements on 9 December 1981 . . . . .	17
9.	Precipitating Proton Energy Spectra Measured by NOAA-6 at Three Selected Latitudes . . . . .	19
10.	Electron Density Profiles Computed from Two Proton Energy Deposition Codes Using the Spectra Shown in Figure 9 . . . . .	20
11.	Average Profiles of Electron Density Produced by Photo- ionization for Three Different Solar Zenith Angles and Four Ranges in the 10.7-cm Solar Flux . . . . .	24

ILLUSTRATIONS (concluded)

12. Energy Flux of Precipitating Electrons that Produce the Same Ionization as Photoionization for Solar Zenith Angles Between $35^\circ$ and $85^\circ$ and 10.7-cm Solar Flux Between 80 and 200. . . . .	25
--	----

## I INTRODUCTION

Ionization in the earth's atmosphere can have significant effects on radio-wave propagation and satellite communications. Adequate compensation of these effects can only be made if the global distribution of ionization can be specified at any instant in time. One of the more promising means by which this global distribution can be estimated is remote sensing. Remote sensing can be done either by directly detecting the ionization or by indirectly specifying the source and then computing the resulting ionization using physical models. At low- and mid-latitudes the primary source of ionization is ultraviolet (UV) radiation from the sun. At high latitudes, the ionization produced by particle precipitation can be comparable to or greater than that produced by solar UV. In general, auroral particle precipitation is highly dynamic so that specification of the sources at high latitudes is extremely complex. Fortunately, however, the most common type of auroral precipitation is also the most steady and spatially uniform. The aurora produced by this steady and spatially uniform precipitation has been referred to as the continuous aurora [Whalen, 1983].

In contrast to the discrete aurora, the continuous aurora is the site of E-region ionization that is fairly constant over scale lengths of tens of kilometers and for times on the order of hours. The continuous aurora has been alternatively referred to as the diffuse aurora or the mantle aurora. The distinction between these terms has been discussed by Whalen [1983]. In general, the continuous aurora is produced by electron and proton precipitation from the central plasma sheet through pitch-angle diffusion [Sharber, 1981]. However, the principal contributors to E-region ionization in the continuous aurora are precipitating electrons with energies of 1 to 10 keV. Winningham et al. [1978], Ling [1981], and Sharber [1981] have discussed the energy spectra of the electrons responsible for the diffuse aurora.

Because it is the most common and widely distributed form of aurora, it is important to understand the continuous aurora in terms of its distribution and its sources. In this paper, we use ground-based radar and satellite measurements to study the characteristics and sources of ionization in the continuous aurora. The radar data were obtained by the incoherent-scatter radar at Chatanika, Alaska. The satellite data include measurements made by the DMSP and NOAA satellites. The data used in this study is described in the next section. We then discuss the characteristics and sources of the continuous aurora using statistical analysis of the radar data as well as case studies involving coordinated satellite measurements.

## II. EXPERIMENTAL TECHNIQUE

The radar data used in this study were obtained by the Chatanika incoherent-scatter radar. The invariant latitude of Chatanika, Alaska is  $64.8^\circ$ , which makes it ideal for studying the continuous aurora in the evening and morning local-time sectors. A useful operating mode for this type of study is an elevation scan in which the radar scans between the north and south horizons in the magnetic meridian plane. Each scan takes 12 to 15 min to complete. Electron density and line-of-sight ion-drift velocity is measured as a function of latitude and altitude. As the earth rotates, the measurements provide a series of meridional cuts through the auroral zone. If the auroral pattern is stationary, both the latitudinal and longitudinal structure of the aurora can be determined.

The meridian scan is also useful for coordinated experiments with polar-orbiting satellites. Polar-orbiting satellites provide measurements as a function of latitude across the auroral zone. These measurements can be directly related to the latitudinal profiles of ionization and electric field deduced from the radar data. In this study, we used data from the DMSP and NOAA satellites. These are polar-orbiting, sun-synchronous satellites that carry instrumentation to measure precipitating particle fluxes. The detectors are sensitive to particles in the energy range that is most important for production of ionization in the auroral E and F regions (hundreds of electron volts to 20 keV). The DMSP satellites data used here consist only of measurements of precipitating electrons. The NOAA satellite data include measurements of precipitating proton flux as well. None of the satellites used in this study are capable of measuring the pitch-angle distribution of the incoming particles. However, electron and proton precipitation in the continuous aurora is fairly isotropic [Sharber, 1981].

### III CHARACTERISTICS OF THE CONTINUOUS AURORA

An example of electron density data obtained during one scan through the continuous aurora is shown in Figure 1. The figure shows contours of constant electron density in the magnetic meridian plan. The horizontal axis is invariant latitude, so that magnetic field lines are approximately vertical. The data in Figure 1 were obtained during a coordinated experiment involving four rocket launches, the Chatanika radar, and the Air Force Geophysics Laboratory's airborne ionospheric observatory. Results of this experiment have been discussed by Swider and Narcissi [1981], Robinson [1982], McMahon et al. [1982], and Strickland and Daniell [1982]. Apparent in the contour plot of Figure 1 are several enhancements in electron density. In the E region, there is an enhancement to the north with a peak density of  $3 \times 10^5$  el/cm<sup>3</sup>. The large latitudinal gradients at the edges of this enhancement indicate that it was probably an auroral arc. In contrast, the E-region ionization south of this arc has a peak density of  $1.4 \times 10^5$  el/cm<sup>3</sup> and has much smaller latitudinal gradients. The latitudinal variation of the weaker enhancement is typical of the continuous aurora. Radar data from scans before and after the one shown confirm the steadiness of this feature. Because it was apparent in contour plots over a period of several hours, we may conclude that this aurora was extended in the east-west direction.

The ionization in the continuous aurora has a characteristic latitudinal distribution that is exemplified in Figure 1. That is, there is usually a single peak in latitude with a symmetric fall-off on either side. This symmetry has been studied by Whalen [1983] who used ionospheric sounder data to show that the latitudinal distribution of ionization is very often Gaussian. By using a chain of sounder stations, Whalen [1983] was able to show that the parameters of the Gaussian do not vary greatly with longitude. Examination of data from successive radar scans confirms the longitudinal homogeneity of the continuous aurora.

is consistent with the conclusions of Sharber [1981] who observed that the latitudinal profile of proton precipitation was approximately Gaussian. Combined with the similarity between the altitude profiles in the electron and proton aurora, we conclude that the ionization produced by the two sources is very similar.

We have used the radar and satellite data for 9 December 1981 to assess the accuracy of two existing codes that compute electron-density profiles from precipitating proton fluxes. One code is based on the work of Rees [1982] who used an empirical approach that assumes continuous energy loss. An alternate formulism has been developed by Jasperse and Basu [1982] using linear transport theory. Our assessment of these codes, however, is not definitive for two reasons. First, the uncertainties in the calibration of the NOAA 6 proton detectors are fairly large. A comparison of the responses of the NOAA 6 detectors with proton detectors on the DMSP F6 satellite during conjunctions of the two vehicles indicate that the fluxes measured by NOAA 6 may be too low by about a factor of two.

The second reason that our comparison is not definitive is that the NOAA 6 satellite was displaced from the radar meridian. Because we cannot say if the local-time variation displayed in Figure 7 is spatial or temporal, the ionization actually produced by the fluxes measured by the satellite is somewhat uncertain. Despite these problems, it is possible to make definite statements about the relative accuracy of the two codes mentioned above.

Examples of three proton spectra measured by NOAA 6 in the 9 December event are shown in Figure 9. They were obtained at three different latitudes within the proton aurora and were chosen to provide an indication of the range of spectra observed in that event. Although spectral information available from the NOAA 6 proton detectors is limited to the proton fluxes at four energies, proton fluxes at other energies are estimated by adding two additional constraints supplied by the satellite measurements. These include the integrated energy flux between 300 eV and 20 keV and the energy at which the proton flux maximizes. The addition of these constraints allows a reasonably accurate reconstruction

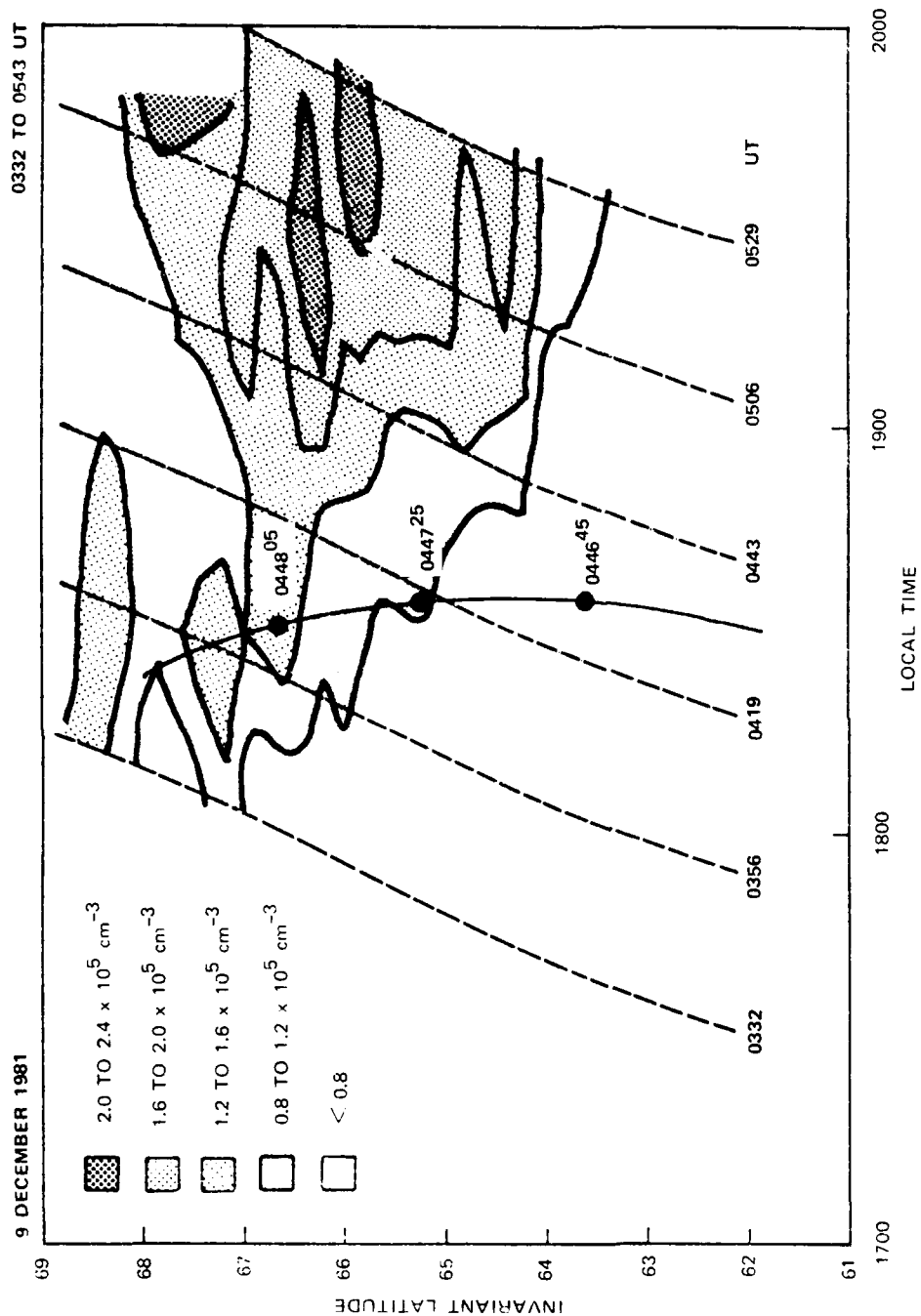


FIGURE 8 ELECTRON DENSITY AT 130-km ALTITUDE AS A FUNCTION OF INVARIANT LATITUDE AND LOCAL TIME CONSTRUCTED FROM RADAR MEASUREMENTS ON 9 DECEMBER 1981



in which the proton fluxes were measured by the NOAA 6 satellite. The upper panel shows the electron density distribution measured by the Chotanika radar at about 1800 local time on 9 December 1981. The NOAA 6 data are shown in the bottom panel. The total energy flux carried by electrons and protons is shown as a function of invariant latitude.

The data show that between  $64^\circ$  and  $68^\circ$  the proton precipitation had an intensity of about  $0.5 \text{ ergs/cm}^2 \text{ s}$ . The corresponding flux carried by electrons in this region is less than  $0.01 \text{ ergs/cm}^2 \text{ s}$ . Comparison with the lower panel in the figure shows that this flux of precipitating protons is comparable to the E-region ionization with a peak of about  $1 \times 10^5 \text{ el/cm}^3$ .

Having identified the ionization measured by the radar during the equator scan beginning at 0332 UT as being produced by proton precipitation, it is possible to follow the development of the proton aurora in the data from subsequent radar scans. Figure 8 summarizes the data from six elevation scans beginning at 0332 UT. The figure shows the electron density at 130-km altitude as a function of invariant latitude and local time. The dashed lines indicate the locations actually sampled by the radar during each scan with the starting time of the scan given at the bottom of the trace. Also shown in the figure is the location of the NOAA 6 satellite pass in invariant-latitude and magnetic-local-time coordinates. The latitudinal range within which protons dominated the precipitation is shown by the cross-hatching superimposed on the trajectory. At the time of the pass, the radar was executing the scan beginning at 1900 local time. Thus, the satellite was displaced one to two hours in local time to the west of the radar.

There are several features to note in Figure 8. First, the equatorward edge of the proton aurora is slanted, extending to lower latitudes at later local times. This slant is consistent with that of the statistical auroral oval. Second, the proton aurora is more intense at later local times. This is either a real spatial variation or is the result of a temporal variation over the two or three hours required by the radar to sample these local times. Finally, the latitudinal variations in the ionization are similar at different local times. That is, the ionization has a central peak with a gradual decrease on either side. This behavior

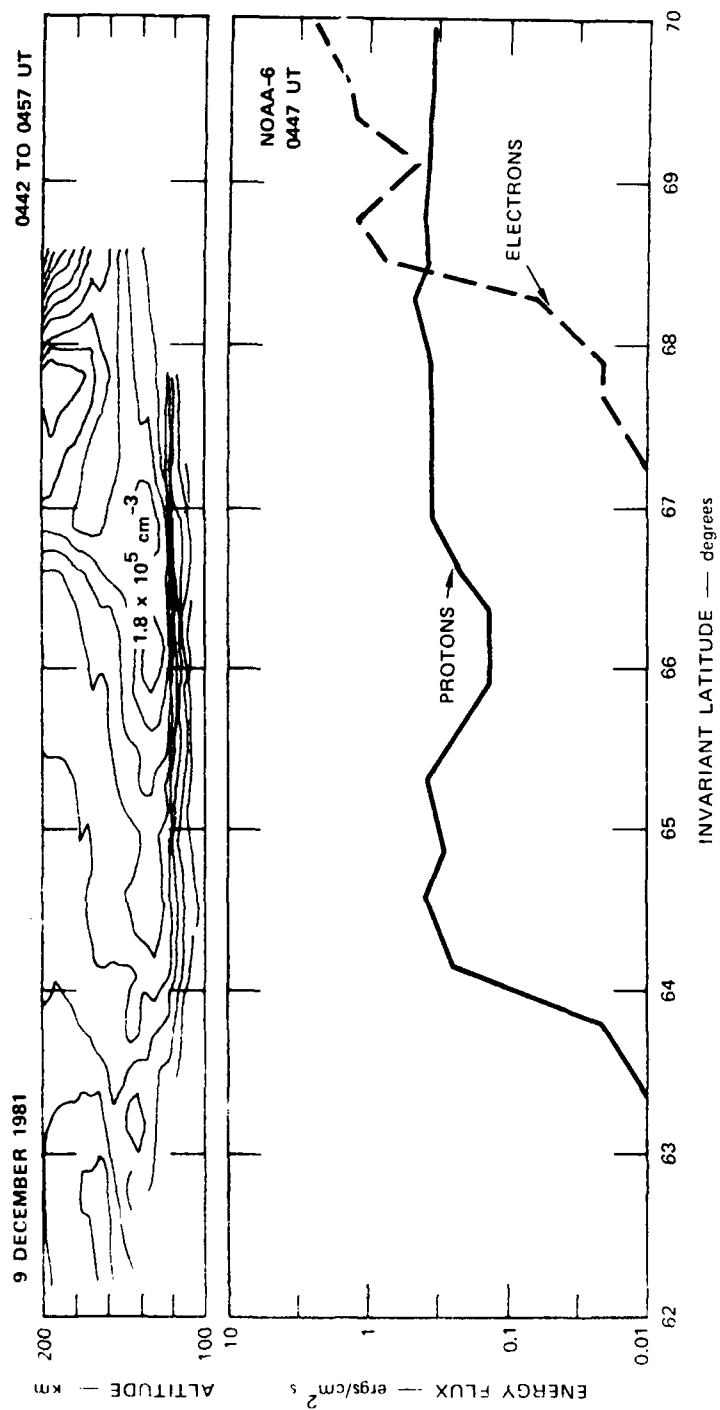


FIGURE 7 A CONTINUOUS AURORAL E-LAYER PRODUCED ENTIRELY BY PRECIPITATING PROTONS

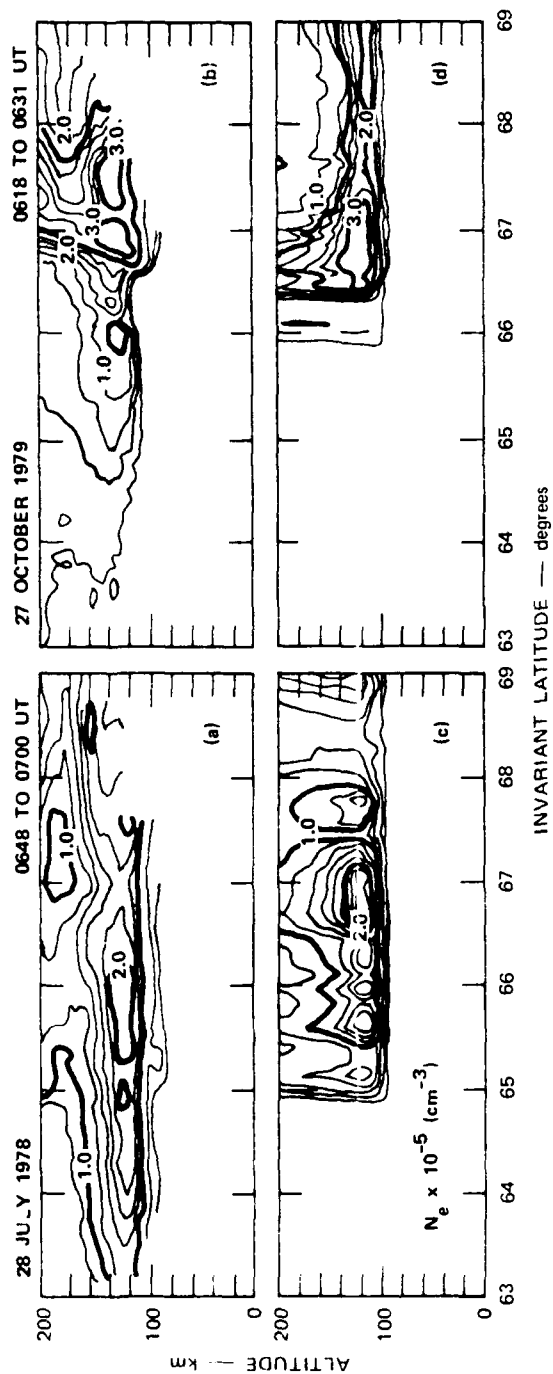


FIGURE 6 TWO EXAMPLES OF CHATANIKA RADAR MEASUREMENTS OF IONIZATION IN PROTON AURORA

contours of electron density computed from the DMSP electron spectrometer data. Only the fluxes of electrons with energies greater than 1 keV were used. The computed profiles agree very well with those measured.

#### B. Protons

The calculations used in Figure 5 have been performed on numerous data sets when good coordinated measurements were available over the continuous aurora. In general, the agreement between calculated and observed ionization is excellent. However, on several occasions the radar data has indicated the presence of significantly more ionization than can be explained by the measured electron fluxes. Examples of two such data sets are shown in Figure 6. Figures 6(a) and 6(b) are electron density contour plots constructed from radar elevation scan data. Figures 6(c) and 6(d) show the electron density derived from simultaneous electron flux measurements from the DMSP F4 satellite, assuming that precipitating electrons were the only source of ionizations. In contrast to Figure 5, these two examples indicate the existence of substantial E-region ionization equatorward of electron precipitation. We attribute the excess ionization to precipitating proton fluxes because protons are the only other significant ionization source in the nighttime ionosphere. In both cases the transition between proton aurora and electron aurora is apparent as a ledge in the lowest altitude contour. Thus, the electron precipitation produces ionization at lower altitudes than the proton precipitation. The ionization within the region of proton precipitation peaks at about  $1 \times 10^5$  el/cm<sup>3</sup> at 130-km altitude. Except for the difference in the altitude of maximum penetration, the two auroras are very similar. This is true also for the latitudinal distribution. The latitudinal variation in peak density in the proton aurora is similar enough to that in the electron aurora that it would be difficult to distinguish the two from ionization measurements alone.

In the above examples the presence of proton precipitation could not be confirmed because of the lack of a proton spectrometer on the DMSP F4 satellite. However, Figure 7 shows an example of a proton aurora

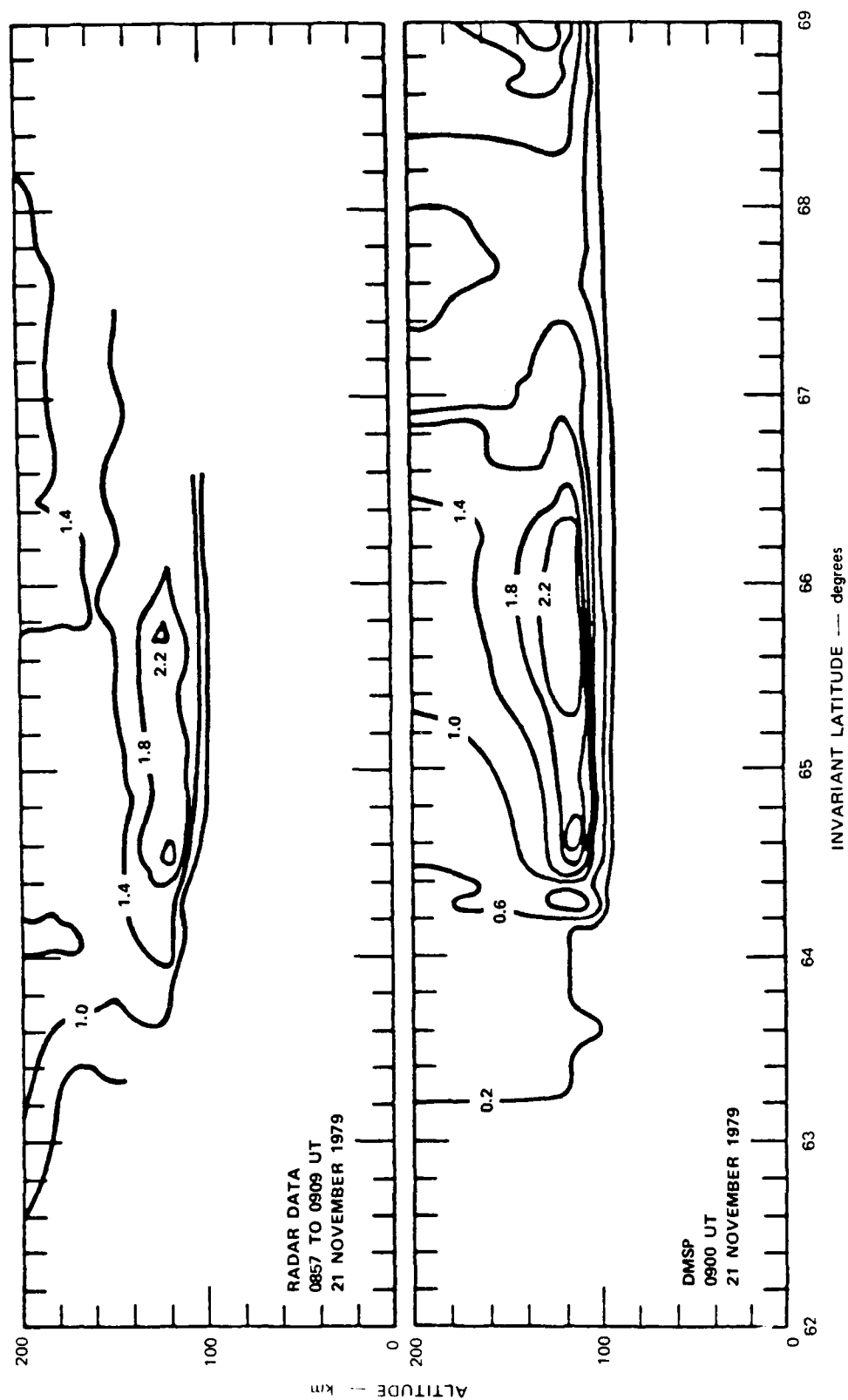


FIGURE 5 COMPARISON OF ELECTRON DENSITY MEASURED BY THE CHATANIKA RADAR WITH THAT COMPUTED FROM SIMULTANEOUS AND COINCIDENT DMSP MEASUREMENTS OF PRECIPITATING ELECTRON FLUXES

auroras. We see immediately that the differences between the two are attributable to the different energy fluxes and characteristic energies of precipitating electrons in these two local-time sectors.

An alternate set of parameters that are useful in characterizing the ionization in the continuous aurora is the height-integrated Hall and Pedersen conductivities computed from the ionization profile. In addition to being useful in estimating the electron source characteristics they also have application to problems in which auroral electrodynamics are important. The relations between Hall and Pedersen conductance and the properties of a Maxwellian electron beam have been described by Vickrey et al. [1981]. These relations indicate that ionization in the evening-sector continuous aurora can be attributed to a source of density between 0.1 and 0.6 el/cm<sup>3</sup> and characteristic energies between 0.8 and 1.6 keV.

An additional ramification of the Maxwellian nature of continuous auroral precipitation is that spectrophotometric techniques for determination of the ionization profile work especially well. These techniques use measurements of auroral emissions at two wavelengths to infer the average energy and energy flux of the precipitating electrons [Rees and Luckey, 1974]. When the incoming spectrum is Maxwellian, the ambiguities involved in these calculations are minimized. Examples of ionization profiles deduced from photometric measurements at two wavelengths have been presented by Vondrak and Sears [1978] and Mende et al. [1984].

The energy deposition codes described above can also be used to reconstruct the altitude profile of ionization from high-altitude measurements of precipitating electron fluxes. Vondrak [1981] has demonstrated the capability of deriving E-region ionization profiles from satellite measurements of electron fluxes. An example of these calculations for electron fluxes measured over a continuous aurora is shown in Figure 5. Contours of electron density measured by the Chatanika radar during an elevation scan in the magnetic meridian plane are shown in the upper panel of the figure. Simultaneous with the scan was a pass of the DMSP F4 satellite. The location of the pass was approximately along the magnetic meridian within 100 km of Chatanika. The bottom panel shows

where  $E_0$  is in keV. The density at the peak is relatively insensitive to characteristic energy but increases as the square root of the energy flux. Approximate expressions relating  $f_o E$  and  $n_{\max} E$  to energy flux independent of the characteristic energy are

$$f_o E = 3.18 \Phi^{\frac{1}{2}} \text{ [MHz]} \quad (2)$$

and

$$n_{\max} E = 1.25 \times 10^5 \Phi^{\frac{1}{2}} \text{ [cm}^{-3}\text{]} \quad (3)$$

where  $\Phi$  is the energy flux in  $\text{ergs/cm}^2 \text{ s}$ . Equation (2) is very close to the relation between  $f_o E$  and energy flux derived experimentally by Sharber [1981].

As a demonstration of the way in which these relations can be used to characterize the continuous aurora, we show in Figure 4 the range in  $h_{\max} E$  and  $n_{\max} E$  observed in the evening- and morning-sector continuous

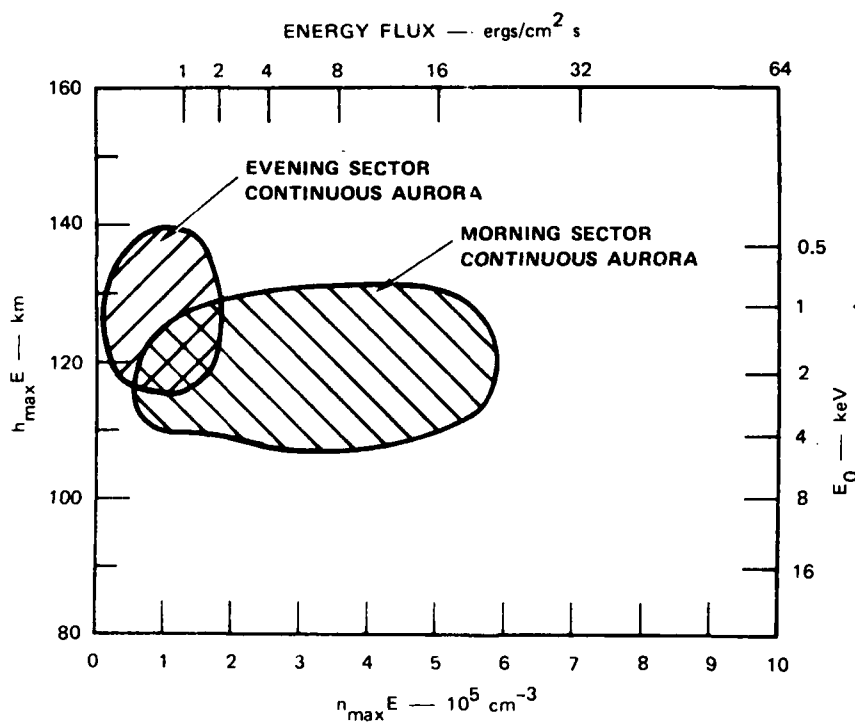


FIGURE 4 COMPARISON OF THE RANGE OF  $n_{\max} E$  AND  $h_{\max} E$  FOUND IN THE MORNING- AND EVENING-SECTOR CONTINUOUS AURORAS

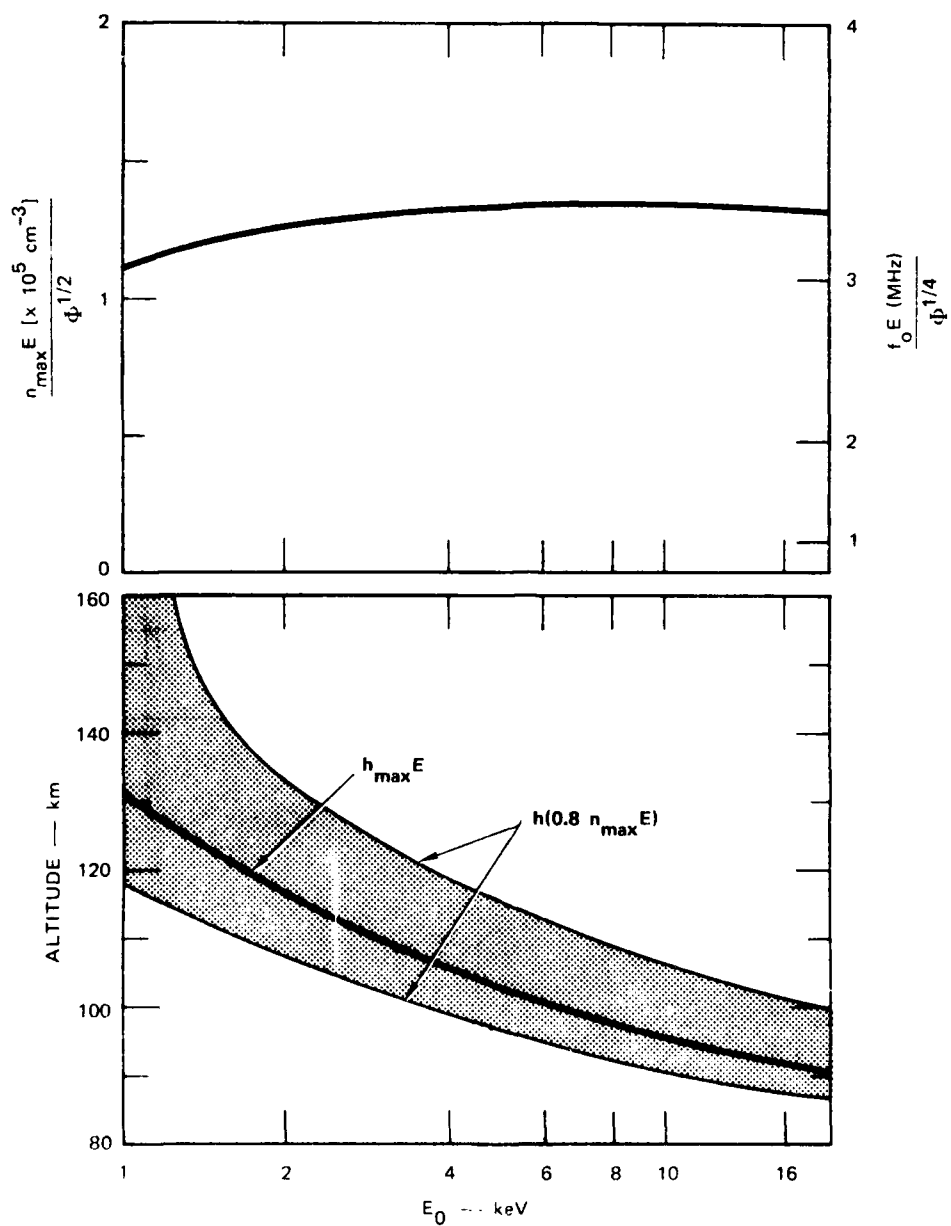


FIGURE 3 CALCULATED VALUES OF  $n_{\max} E$ ,  $f_o E$ , AND  $h_{\max} E$  RESULTING FROM PRECIPITATING ELECTRONS WITH MAXWELLIAN ENERGY DISTRIBUTIONS



#### IV SOURCES OF THE CONTINUOUS AURORA

##### A. Electrons

Sharber [1981] presented ISIS 2 satellite data to show that the continuous aurora is primarily produced by precipitating electrons whose differential number spectrum is approximately Maxwellian for energies greater than about 1 keV. We can calculate the ionization profile produced by precipitating electrons in the altitude range up to about 200 km using any of several auroral energy deposition codes [Rees, 1963; Walt et al., 1969; Berger et al., 1970; Banks et al., 1974; Jasperse and Strickland, 1981]. An example is shown by the solid curve in Figure 2, which was computed using a Maxwellian energy spectrum with a characteristic energy ( $E_0$ ) of 1 keV and an energy flux ( $\Phi$ ) of  $2 \text{ ergs/cm}^2\text{s}$ . The resulting profile is very similar to those observed.

The significance of the Maxwellian nature of precipitation in the continuous aurora is that the spectrum and the resulting ionization profile can be uniquely described by two parameters. For example, a useful set of parameters is the electron density at the E-region peak ( $n_{\text{max}}^{\text{E}}$ ) and the altitude of the peak ( $h_{\text{max}}^{\text{E}}$ ). Figure 3 shows  $f_o^{\text{E}}$ ,  $n_{\text{max}}^{\text{E}}$ , and  $h_{\text{max}}^{\text{E}}$  as a function of the characteristic energy of the Maxwellian. The calculations were done using an energy deposition code based on the technique described by Rees [1963]. The results show that the height of the maximum E-region density depends only on the characteristic energy. The altitudes above and below the peak at which the density falls to 80 percent of the peak density are also shown. For smaller values of  $E_0$ , the peaks are broader and higher. An approximate expression relating  $h_{\text{max}}^{\text{E}}$  to characteristic energy independent of energy flux is

$$h_{\text{max}}^{\text{E}} = -13.6 \ln(E_0) + 128 \text{ [km]} \quad (1)$$

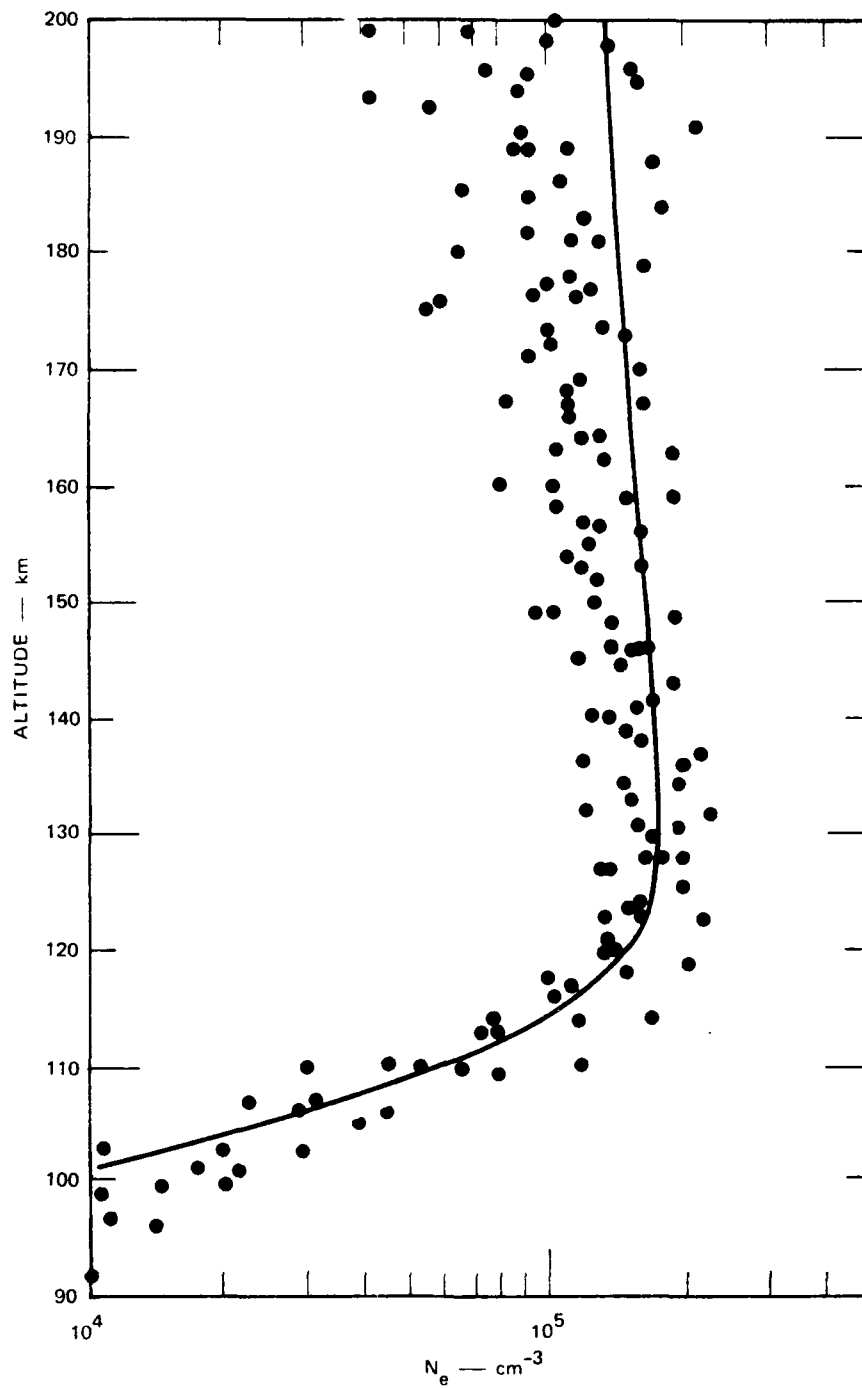


FIGURE 2 SUPERIMPOSED ELECTRON DENSITY MEASUREMENTS  
FROM THE AURORA SHOWN IN FIGURE 1

The altitude distribution of ionization in the continuous aurora is shown in Figure 2, in which data from five profiles in Figure 1 have been superimposed. The range in  $n_{\text{max}}^{\text{E}}$  is from 1 to  $2 \times 10^5 \text{ el/cm}^3$ . The altitude of peak density,  $h_{\text{max}}^{\text{E}}$ , is from 120 to 140 km. The peak is often broad and difficult to identify. Below the peak the ionization falls off rapidly while above the peak a much slower decrease is observed. Electron densities in the continuous aurora below 90 km are usually less than  $10^4 \text{ el/cm}^3$ .

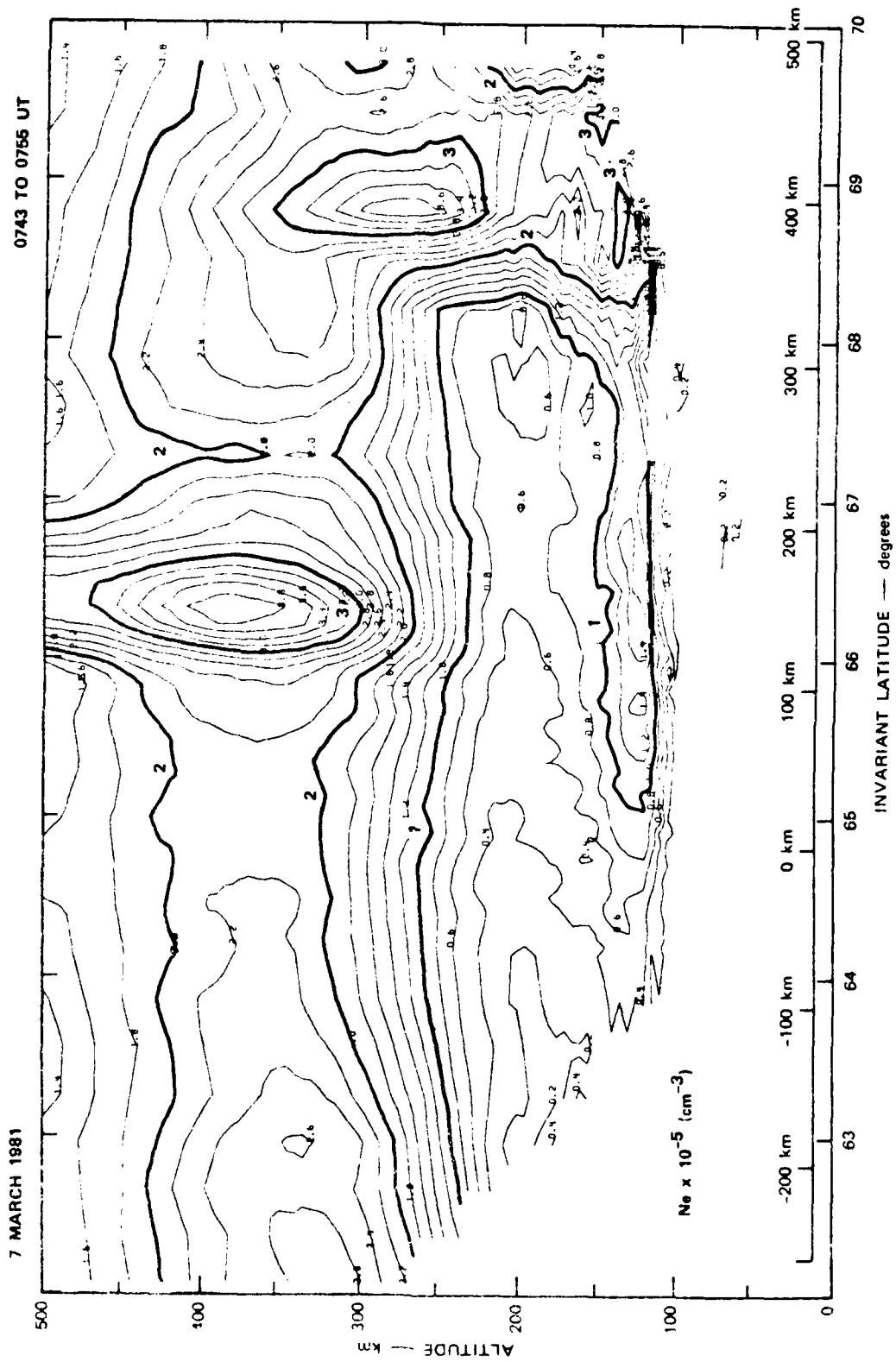


FIGURE 1 ELECTRON DENSITY AS A FUNCTION OF LATITUDE AND ALTITUDE MEASURED BY THE CHATANIKA RADAR ON 7 MARCH 1981

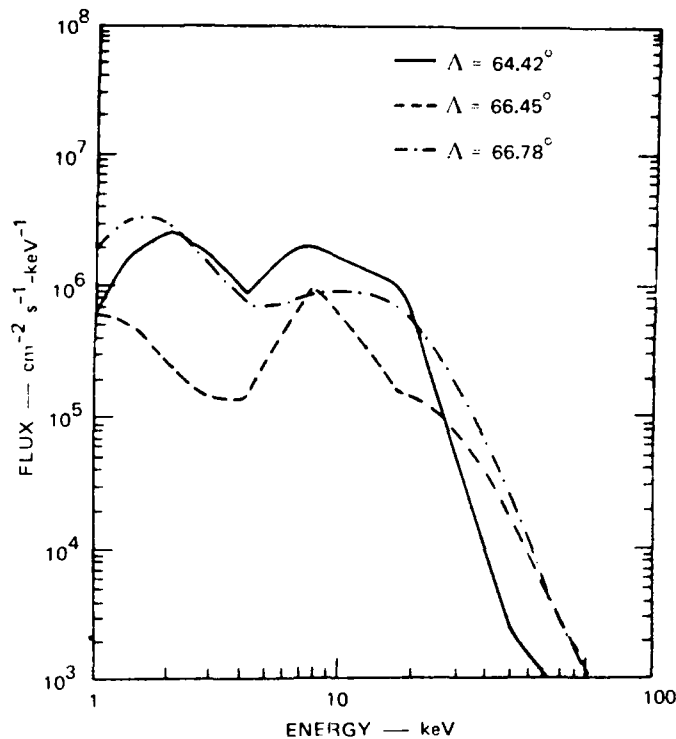


FIGURE 9 PRECIPITATING PROTON ENERGY SPECTRA MEASURED BY NOAA-6 AT THREE SELECTED LATITUDES

of the actual spectrum. The spectra shown in Figure 9 are approximately Maxwellian with temperatures between 5 and 7 keV. The energy flux varies between 0.1 and 0.6 ergs/cm<sup>2</sup>s.

Electron density profiles computed from the two codes using these three spectra as input are shown in Figure 10 (a), (b), and (c). Also shown in Figure 10 are electron density profiles measured by the radar in the proton aurora. Because of the displacement between the radar meridian and the satellite ground track, the correct profile to use for comparison cannot be determined. Rather than try to choose a profile at the same invariant latitude, we chose instead profiles whose peak densities were approximately equal to those computed from the codes. For profiles in which the peak densities computed with the two codes did not agree, we chose a profile with peak density equal to the average of the two. Although this selection process is somewhat arbitrary, it allows us to make some statements about the accuracy of each model. In particular, we note from Figure 10 that the code based on linear transport theory models the decrease in density with altitude above the peak much more

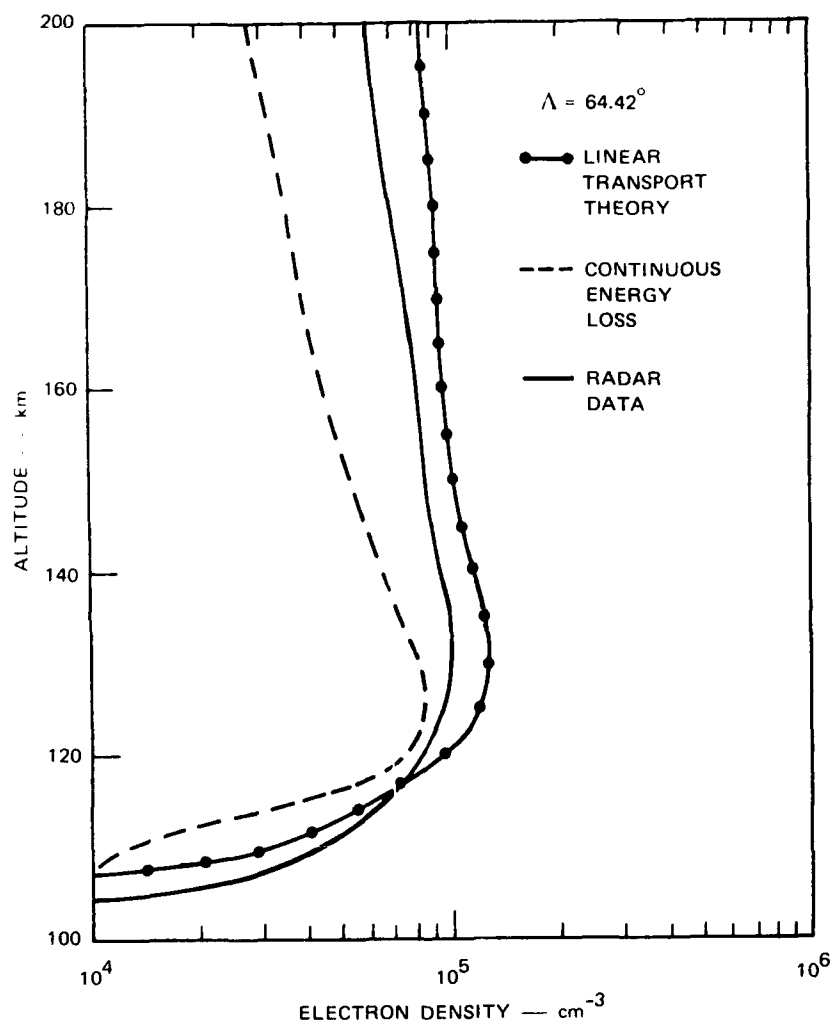


FIGURE 10 ELECTRON DENSITY PROFILES COMPUTED FROM TWO PROTON ENERGY DEPOSITION CODES USING THE SPECTRA SHOWN IN FIGURE 9

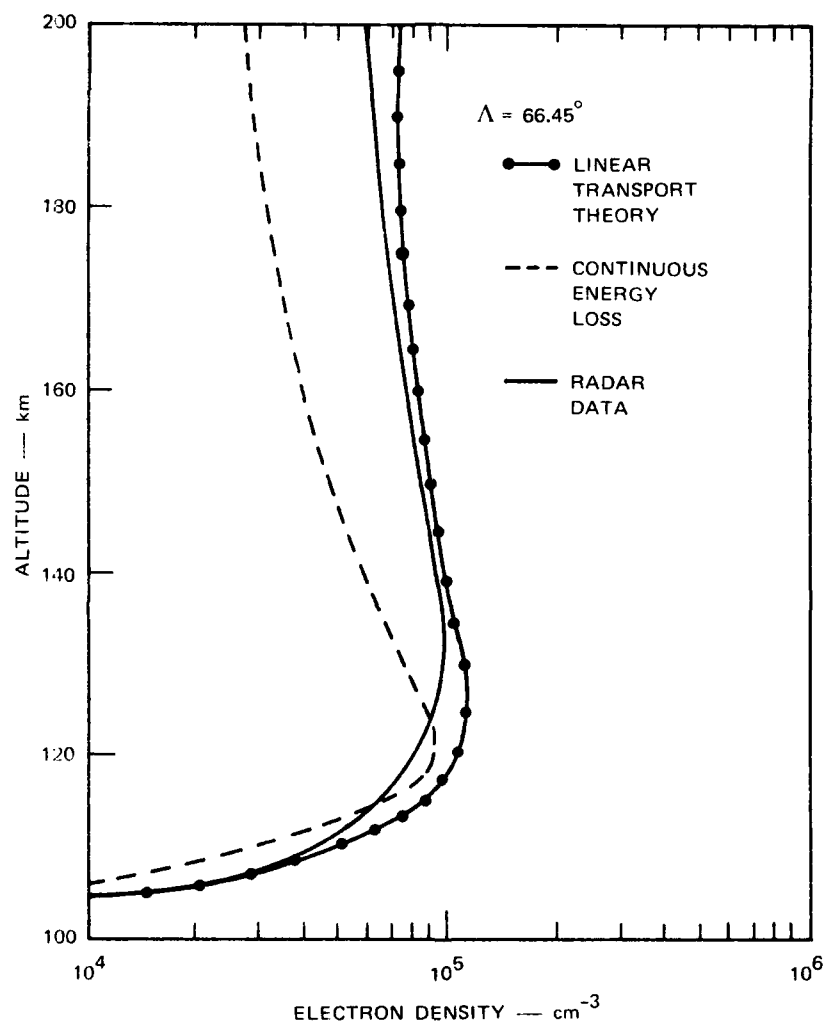


FIGURE 10 (continued)

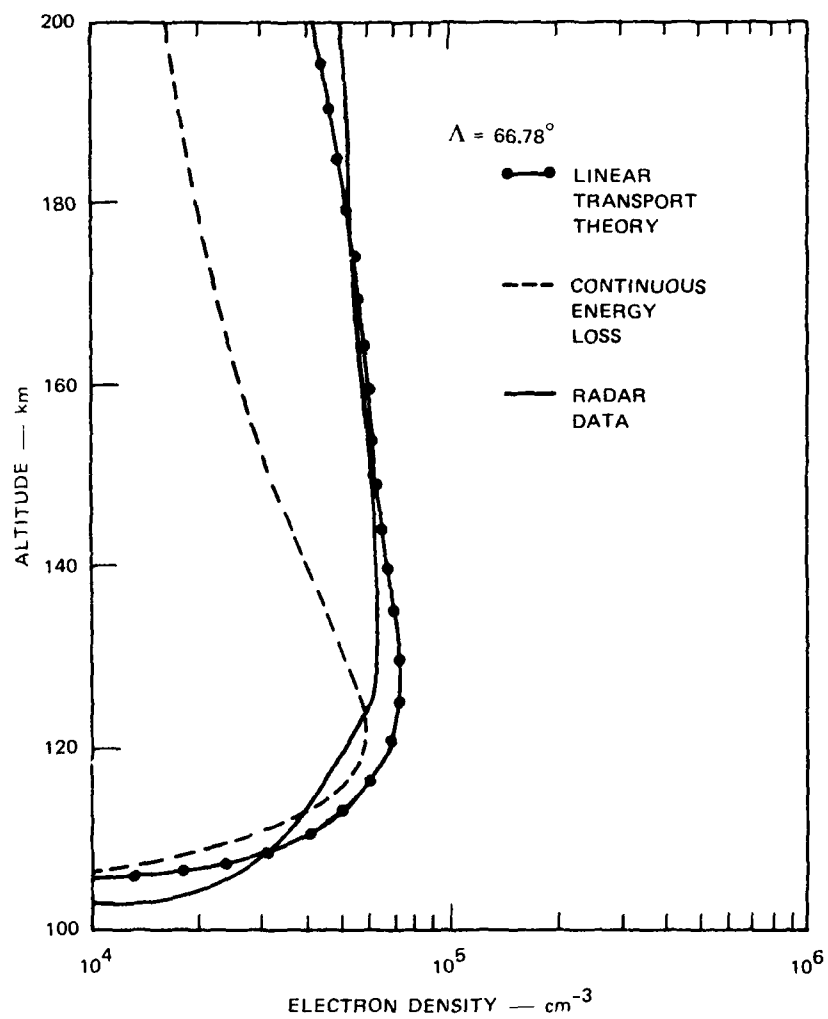


FIGURE 10 (concluded)



accurately than the continuous energy loss approach. In addition, the continuous energy loss approach yields E-region peak altitudes significantly lower than those indicated by the radar profiles. Thus, this comparison indicates that the linear transport theory gives a more accurate representation of the altitude distribution of ionization produced by precipitating protons.

### C. Photoionization

A third possible source of continuous E-region ionization is photoionization. To assess the contribution from this source, we examined Chatanika radar data obtained on 12 different days during the past ten years [Robinson and Vondrak, 1984]. To study the ionization produced exclusively by photoionization, we chose magnetically quiet days that ensured the absence of particle precipitation. We sorted the data according to solar zenith angle and solar flux. Four solar flux categories were defined based on the 10.7-cm solar flux:  $S_a = 80$  to 120,  $S_a = 120$  to 160,  $S_a = 160$  to 200, and  $S_a = 200$  to 240. The result of averaging the profiles within each bin is shown in Figure 11. Average profiles for each of the four solar flux intervals are shown for solar zenith angles of  $45^\circ$ ,  $65^\circ$ , and  $85^\circ$ . These results show that for solar zenith angles less than  $65^\circ$ , photoionization produces E-region densities comparable to those observed in the continuous aurora. Also, the ionization at the E-region peak can change by more than a factor of two between the lowest and highest levels of solar flux.

We compare the ionization produced by solar illumination to the equivalent flux of precipitating electrons in Figure 12. During the maximum years of the solar cycle, when the 10.7-cm solar flux can exceed 200, photoionization can be as effective in ionizing the E region as an electron beam of  $1 \text{ erg/cm}^2 \text{ s}$ , even for solar zenith angles as large as  $75^\circ$ . At a geographic latitude of  $70^\circ$  in summer, the solar zenith angle is less than  $75^\circ$  for most of the day. Because the ionization produced by solar illumination varies slowly with latitude, this source can produce ionization in the E region with a latitudinal distribution similar to that in the continuous aurora.

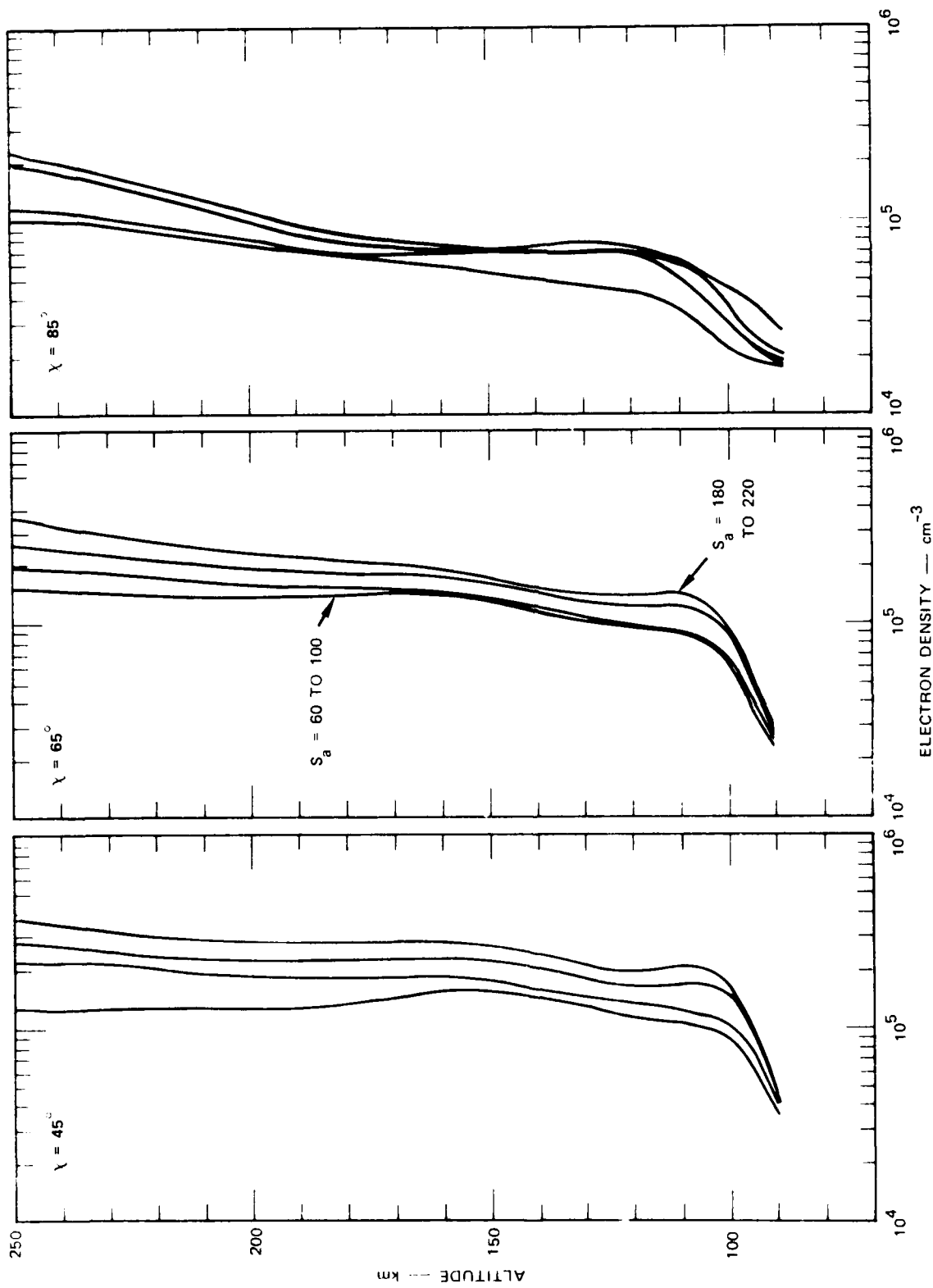


FIGURE 11 AVERAGE PROFILES OF ELECTRON DENSITY PRODUCED BY PHOTOIONIZATION FOR THREE DIFFERENT SOLAR ZENITH ANGLES AND FOUR RANGES IN THE 10.7-cm SOLAR FLUX

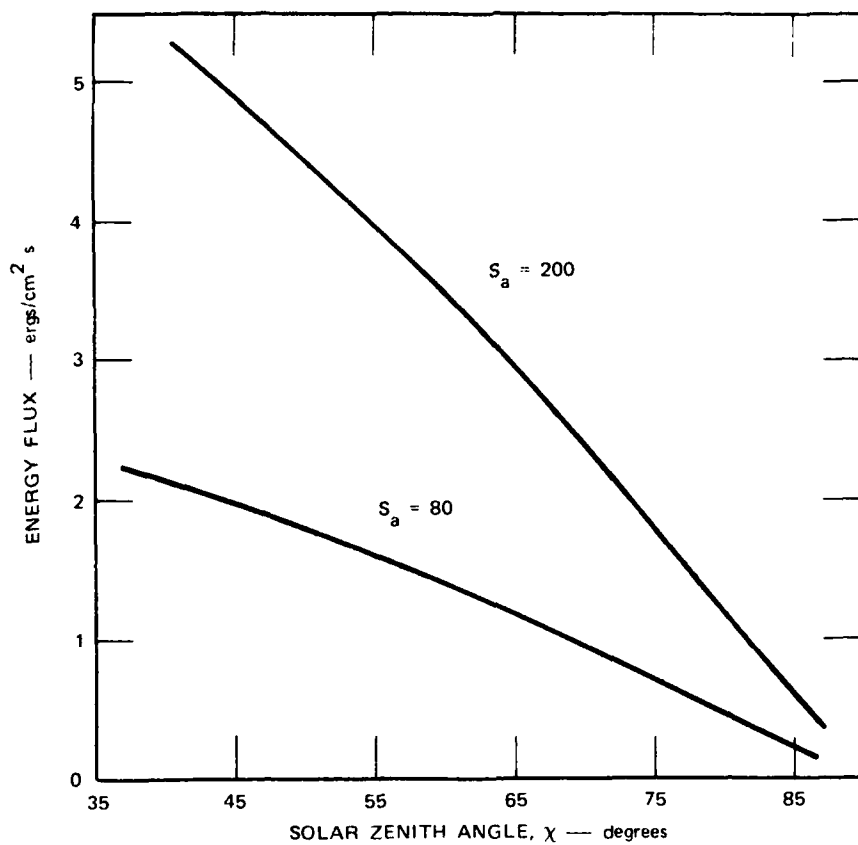


FIGURE 12 ENERGY FLUX OF PRECIPITATING ELECTRONS THAT PRODUCE THE SAME IONIZATION AS PHOTOIONIZATION FOR SOLAR ZENITH ANGLES BETWEEN  $35^\circ$  AND  $85^\circ$  AND 10.7-cm SOLAR FLUX BETWEEN 80 AND 200

## V CONCLUSIONS

Although precipitating electrons account for most of the ionization in the continuous aurora, other sources may also be present that contribute comparably to E-region electron density. Proton precipitation can produce an E region with densities greater than  $10^5$  el/cm<sup>3</sup> at altitudes between 120 and 130 km. In the examples shown here, this occurred close to local dusk at latitudes equatorward of the electron precipitation. However, we have little information about what combination of circumstances create such intense fluxes. Photoionization can also produce E-region densities comparable to those found in the continuous aurora.

The ionization produced by these three sources can be fairly accurately determined when information is available about the intensity of the source. For precipitating electrons, a straightforward energy deposition code can be used to compute the electron density profile between 90- and 160-km altitude. Because the energy distribution of precipitating electrons is approximately Maxwellian, accurate spectral information can be obtained by spectrophotometric techniques. For precipitating protons, further testing of the codes that compute altitude profiles of ionization from proton spectral information needs to be performed. Our preliminary analysis indicates that linear transport theory provides more accurate results than codes based on continuous energy loss. Precipitating proton energy spectra are also approximately Maxwellian. However, spectrophotometric techniques for determining the parameters of the Maxwellian have yet to be developed. Finally, ionization produced by solar illumination depends on solar zenith angle and F 10.7-cm solar flux. A statistical study based on Chatanika radar data indicates that the altitude profile of ionization from photoionization can be accurately determined from these two quantities.

#### REFERENCES

- Banks, P. M., C. R. Chappel, and A. F. Nagy, "A New Model of the Interaction of Auroral Electrons with the Atmosphere: Spectral Degradation, Backscatter, Optical Emission, and Ionization," J. Geophys. Res., 79, 1459, 1974.
- Berger, M. J., A. M. Seltzer, and K. Maeda, "Energy Deposition by Auroral Electrons in the Atmosphere," J. Atmos. Terr. Phys., 32, 1015, 1970.
- Jasperse, J. R., and B. Basu, "Transport Theoretic Solution for Auroral Proton and H Atom Fluxes and Related Quantities," J. Geophys. Res., 87, 811, 1982.
- Jasperse, J. R., and D. J. Strickland, "Approximate Analytic Solutions for the Primary Auroral Electron Flux and Related Quantities," AFGL-TR-81-0069, Air Force Geophysics Laboratory, Hanscom AFB, MA, 1981, ADA102905.
- McMahon, W. J., L. Heroux, and R. H. Salter, "Electron and Proton Spectrometry in the AFGL Auroral E Program, I. Experiment Overview and Preliminary Auroral Electron Data," Internal Report, AFGL-TR-82-0121, Air Force Geophysics Laboratory, Hanscom AFB, MA, 1982, ADA120861.
- Mende, S. B., R. H. Eather, M. H. Rees, R. R. Vondrak, and R. M. Robinson, "Optical Mapping of Ionospheric Conductance," J. Geophys. Res., 89, 1755, 1984.
- Meng, C.-I., "Electron Precipitation in the Midday Auroral Oval," J. Geophys. Res., 86, 149, 1981.
- Rees, M. H., "Auroral Ionization and Excitation by Incident Energetic Electrons," Planet. Space Sci., 11, 1209, 1963.
- Rees, M. H., "On the Interaction of Auroral Protons with the Earth's Atmosphere," Planet. Space Sci., 30, 463, 1982.

REFERENCES (continued)

- Rees, M. H., and D. Luckey, "Auroral Electron Energy Derived from Ratio of Spectroscopic Emissions: 1. Model Computations," J. Geophys. Res., 79, 5181, 1974.
- Robinson, R. M., "Chatanika Radar Measurements of the Continuous Aurora," Final Report, AFGL-TR-82-0297, Air Force Geophysics Laboratory, Hanscom AFB, MA, 1982, ADA124023.
- Robinson, R. M., and R. R. Vondrak, "Measurements of E-Region Ionization and Conductivity Produced by Solar Illumination at High Latitudes," J. Geophys. Res., in press, 1984.
- Sharber, J. R., "The Continuous (Diffuse) Aurora and Auroral-e Ionization," in Physics of Space Plasmas, T. S. Chang, B. Coppi, and J. R. Jasperse eds., SRI Conference Proceedings and Reprint Series, Vol. 7 (Scientific Publishers, Cambridge, MA, 1981).
- Strickland, D. J., and R. E. Daniell, "UV Emissions and the Electron Density in the Auroral and Low- to Mid-Latitude Daytime Ionospheres," Final Report, AFGL-TR-82-0373, Air Force Geophysics Laboratory, Hanscom AFB, MA, 1982, ADA126318.
- Swider, W., and R. S. Narcisi, "Problems with the  $N_2^+ + O \rightarrow NO^+ + N$  Reaction in Aurora," Geophys. Res. Lett., 8, 1239, 1981.
- Vickrey, J. F., R. R. Vondrak, and S. Matthews, "The Diurnal and Latitudinal Variation of Auroral-Zone Ionospheric Conductivity," J. Geophys. Res., 86, 65, 1981.
- Vondrak, R. R., "Remote Sensing of High Latitude Ionization Profiles by Ground-Based and Spaceborne Instrumentation," in Effect of the Ionosphere on Radiowave Systems, John Goodman, ed., Proceedings of Ionospheric Effects Symposium, Alexandria, VA, 1981.
- Vondrak, R. R., and R. D. Sears, "Comparison of Incoherent Scatter Radar and Photometric Measurements of the Energy Distribution of Auroral Electrons," J. Geophys. Res., 83, 1665, 1978.

REFERENCES (concluded)

- Walt, M., W. M. MacDonald, and W. E. Francis, "Penetration of Auroral Electrons into the Atmosphere," in Physics of the Magnetosphere, R. L. Carollano, ed. (D. Reidel, Dordrecht, Netherlands, 1969).
- Whalen, J. A., "A Quantitative Description of the Spatial Distribution and Dynamics of the Energy Flux in the Continuous Aurora," J. Geophys. Res., 88, 7155, 1983.
- Winningham, J. D., C. D. Anger, G. G. Shepherd, E. J. Weber, and R. A. Wagner, "A Case Study of the Aurora, High-Latitude Ionosphere, and Particle Precipitation During Near-Steady State Conditions," J. Geophys. Res., 83, 5751, 1978.

**END**

**FILMED**

**7-85**

**DTIC**